UNCLASSIFIED

DEFENCE RESEARCH ESTABLISHMENT
CENTRE DE RECHERCHES POUR LA DÉFENSE
VALCARTIER, QUÉBEC

DREV TM 1999-220
Unlimited Distribution / Distribution illimitée

IMPROVED IMAGE CORRECTION TECHNIQUE FOR VISUALIZATION OF THE AIR/FUEL MIXING IN A DUCTED ROCKET COMBUSTOR

by

M.A. Jeffries and R.A. Stowe

March/mars 2000

Approved by/approuvé par
Paul Harris for
Head, Delivery Systems Section
Chef, Section systèmes de lancement

30/3/2000
Date

SANS CLASSIFICATION

ABSTRACT

The Defence Research Establishment Valcartier (DREV) in Canada and the TNO Prins Maurits Laboratory (TNO-PML) in the Netherlands have undertaken a collaborative activity known as the Integral Rocket Ramjet Demonstration Program (IRRDP) to demonstrate several of the key technologies of an airbreathing propulsion unit for a medium-range air-launched missile. An essential component of the airbreathing propulsion system is the ducted rocket combustor and, as part of its development, extensive visualization of the simulated air/fuel mixing has been done using plexiglass models within a water tunnel. Images of simulated fuel concentration were used to validate computational fluid dynamic (CFD) modelling of the same combustor, but unfortunately only qualitative comparisons were possible because of effects from several optical phenomena. Improved optics and image correction techniques to account for the various optical phenomena have yielded more quantitative results of simulated fuel concentration within the combustor. Comparisons of time-averaged, corrected images to the CFD results have been very encouraging for some of the configurations studied.

RÉSUMÉ

Le Centre de recherches pour la défense Valcartier (CRDV) au Canada et le TNO Prins Maurits Laboratory (TNO-PML) aux Pays-Bas ont participé à une activité de collaboration appelée "Integral Rocket Ramjet Demonstration Program" (IRRDP) afin de présenter certaines technologies importantes d'un moteur à propulsion aérobie pour un missile de moyenne portée lancé à partir d'une plate-forme aérienne. Une des composantes essentielles du système à propulsion aérobie est le foyer de combustion de la statofusée. Durant une partie de ce développement, nous avons visualisé l'écoulement dans un modèle en plexiglass du foyer de combustion dans un tunnel à eau. Des images de la concentration de carburant simulé ont été utilisées afin de valider la modélisation numérique de l'écoulement (CFD) du même foyer de combustion, mais on n'a pu effectuer que des comparaisons qualitatives furent possibles. Les composantes optiques et les techniques de correction des images tenant compte des multiples phénomènes optiques ont été mis au point pour donner des résultats plus quantitatifs de la concentration de carburant simulé dans le foyer de combustion. Des comparaisons de la moyenne basée sur le temps de quelques images corrigées avec les résultats de CFD étaient très encourageantes pour certaines des configurations étudiées.

IRRDP Follow-on

INTEGRAL ROCKET RAMJET DEMONSTRATION PROGRAM FOLLOW-ON

Defence Research Establishment Valcartier
2459 Pie-XI Blvd. North, Val-Bélair, Québec, Canada, G3J 1X5

TNO Prins Maurits Laboratory
P.O. Box 45, 2280 AA Rijswijk, the Netherlands

Title of Document: IMPROVED IMAGE CORRECTION TECHNIQUE FOR VISUALIZATION OF AIR/FUEL MIXING IN A DUCTED ROCKET COMBUSTOR

IRRDP Document: IRRDP-DREV-TN-9902(1)
DREV Document: DREV TM 1999-220
Date: 01-03-2000
Work package: 400

	Name	Signature	Date
Authors	M.A. Jeffries	R Stowe for M. Jeffries	23/03/00
	R.A. Stowe	R Stowe	23/03/00
Checked	G. Roy	G Roy	23.03.2000
Approved	G. Dumas	G Dumas	30/3/2000

Warning Notice

© Her Majesty the Queen in the Right of Canada as represented by the Minister of National Defence, 2000. The information contained herein is proprietary to Her Majesty and is provided to the recipient on the understanding that it will be used for information and evaluation purposes only. Any commercial use including use for manufacture is prohibited. Release to third parties of this publication or of information contained herein is prohibited without the prior written consent of DND Canada.

© TNO Prins Maurits Laboratory, all rights reserved. No part of this document may be reproduced in any form, by print, photoprint, microfilm, or any other means without permission of TNO. Disclosure to third parties of this document or any part thereof, or the use of this document by persons other than persons who have a need to know any information contained herein, is prohibited.

Distribution

The complete distribution list is included at the end of the document.

TABLE OF CONTENTS

	ABSTRACT/RÉSUMÉ	i
	EXECUTIVE SUMMARY	v
1.0	INTRODUCTION	1
2.0	RAMJET TECHNOLOGY AND DUCTED ROCKETS	3
3.0	WATER TUNNEL AND OPTICAL SETUP	4
4.0	DETERMINATION OF MASS FLOW RATES	8
5.0	CFD MODELLING	10
6.0	FINAL IMAGE CORRECTION TECHNIQUE	11
7.0	REYNOLDS NUMBER EFFECTS	14
8.0	WATER TUNNEL AND CFD COMPARISON	15
9.0	CONCLUSIONS AND RECOMMENDATIONS	21
10.0	ACKNOWLEDGEMENTS	23
11.0	REFERENCES	24
	FIGURES 1 to 22	
	TABLE I	

EXECUTIVE SUMMARY

The Defence Research Establishment Valcartier (DREV) in Canada and the TNO Prins Maurits Laboratory (TNO-PML) in the Netherlands have undertaken a collaborative activity known as the Integral Rocket Ramjet Demonstration Program (IRRDP) to study the use of a ducted rocket for missile propulsion. The overall goal is to develop a technology base for the Canadian and Dutch Armed Forces suitable for threat assessment, future weapons evaluation, and participation in multi-national missile development programs. Currently, tactical missiles in the inventories of both countries rely heavily, if not exclusively, on solid fuel rockets for propulsion. However, a ducted rocket has several advantages over solid fuel rocket motors, including increased range, higher speed, and throttleability, with only a limited increase in complexity.

An essential component of the airbreathing propulsion system is the ducted rocket combustor. As part of its development, extensive visualization of the simulated air/fuel mixing within various combustor geometries and test conditions has been done using plexiglass models within a water tunnel. Images of simulated fuel concentration were used to validate computational fluid dynamic (CFD) modelling of the same combustor, but unfortunately only qualitative comparisons were possible because of effects from several optical phenomena. These phenomena include Mie scattering of the laser light from the seed bubbles which represented the fuel, the Gaussian intensity profile of the laser sheet, attenuation, optical distortion of the image due to changes in the indices of refraction of the various media, and reflections from the plexiglass model. To better understand the air/fuel mixing and validate the CFD, a more quantitative picture of the simulated fuel concentration within the combustor is desired. We have now developed an improved technique to correct raw images from the water tunnel and, while not yet optimized for all configurations, allows for more direct comparison with CFD results.

This improved technique included modifications to the optics used to generate the laser sheet and an improved computer program written in FORTRAN to correct the raw images for the most important of the optical phenomena. Basically, this program made the seed bubble concentration in the model directly proportional to the pixel intensity and rescaled the corrected images from 0 to 100% fuel. To overcome the time-dependence of the flow phenomena, ten sequential, corrected and rescaled images were averaged to be more comparable to the quasi-steady CFD images. These averaged images provide a quantitative fuel concentration comparison with CFD modelling.

Results for comparison between the water tunnel images and CFD were good for some configurations, but not all. Further improvements to the seeding and correction techniques will be necessary to ensure more consistent results. With these improvements the water tunnel image correction technique could be a useful tool to quantitatively validate CFD results for ducted rocket and other types of combustors.

1.0 INTRODUCTION

The Defence Research Establishment Valcartier (DREV) in Canada and the TNO Prins Maurits Laboratory (TNO-PML) in the Netherlands have undertaken a collaborative activity known as the Integral Rocket Ramjet Demonstration Program (IRRDP) to study the use of a ducted rocket for missile propulsion. The overall goal is to develop a technology base for the Canadian and Dutch Armed Forces suitable for threat assessment, future weapons evaluation, and participation in multi-national missile development programs. Currently, tactical missiles in the inventories of both countries rely heavily, if not exclusively, on solid fuel rockets for propulsion. However, a ducted rocket has several advantages over solid fuel rocket motors, including increased range, higher speed, and throttleability, with only a limited increase in complexity.

An essential component of the airbreathing propulsion system is the ducted rocket combustor. As part of its development, extensive visualization of the simulated air/fuel mixing within various combustor geometries and test conditions has been done using plexiglass models within a water tunnel. Images of simulated fuel concentration were used to validate computational fluid dynamic (CFD) modelling of the same combustor, but unfortunately only qualitative comparisons were possible because of effects from several optical phenomena. To better understand the air/fuel mixing and validate the CFD, a more quantitative picture of the simulated fuel concentration within the combustor is desired. We have now developed an improved technique to correct raw images from the water tunnel and, while not yet optimized for all configurations, allows for more direct comparison with CFD results.

The main advantage of using a water tunnel to visualize the flow inside a combustor is that with water as the working fluid, the Reynolds numbers obtained are representative of those obtained in an actual ducted rocket combustor, but fluid velocities are on the order of 1 m/s. At these low velocities, the flow phenomena can be easily recorded using a video camera at an appropriate shutter speed. In DREV's water tunnel, water is used to simulate both the air and the fuel, and is pumped into a 100-mm diameter plexiglass model combustor. Cavitation bubbles, induced by injecting a small amount of high-pressure water

into the fuel line, are used to seed the simulated fuel flow so that it could be differentiated from the simulated air. By passing a laser sheet down the central longitudinal plane of the combustor, an image of the concentration field can be captured with a digital video camera. The laser light scatters off the cavitation bubbles and is detected by the pixels of the charge-coupled device (CCD) in the video camera to produce a raw image of the configuration.

Unfortunately, there are several optical phenomena that prevent the raw images from being compared directly with the CFD results. The scattering of the laser light from the cavitation bubbles (Mie scattering) is very dependent on angle. It is much greater in the forward than the backward direction that leads to a biased image that is much more intense on one side than the other. The Gaussian intensity profile of the laser beam and consequently the laser sheet means that there is more intense light in the middle and less at the extremities. The laser light is also attenuated the further away it is from the laser. Other factors were optical distortion of the image from changes in the indices of refraction of the various media, reflections from the plexiglass model (particularly from where the air inlets intersect the main combustor body), and effects of multiple scattering. No corrections were made for optical distortion (which was small, Ref. 1) nor reflections, and multiple scattering effects were assumed to be minimal since the concentration of cavitation bubbles was low. However, by correcting the raw images for variations in the vertical and horizontal directions and rescaling them from 0% to 100% fuel to correct for background light, the pixel value of the image is assumed to be directly proportional to the fuel concentration. These corrected images could then be more directly and quantitatively compared with the CFD results. In previous studies (Refs. 1 and 2) this was not done, so only qualitative comparisons between the CFD and water tunnel results could be made.

A further complicating point is that turbulent fluid flow is a highly time-dependent phenomenon. Each video image taken during the water tunnel experiments is therefore a snapshot of the flow, averaged only over the time the shutter is open. However, using CFD with a turbulence model results in a time-averaged result for the flow phenomena, so this time-dependence is not evident. To overcome this difference between the water tunnel and CFD results, several images were then averaged to obtain a less time-dependent view

of the flowfield. The focus of this project was therefore to improve the laser sheet and image correction technique so corrected and rescaled images, once time-averaged, could be compared more accurately and quantitatively with the CFD modelling.

This work was carried out at DREV between April and August 1999 under Work Unit 3eb13, Airbreathing Propulsion Feasibility.

2.0 RAMJET TECHNOLOGY AND DUCTED ROCKETS

Over the past few years, ramjets have been gaining favour for missile propulsion over solid propellant rocket motors. The main reason is that rather than carrying its oxidizer onboard like a rocket motor, a ramjet uses air from the surrounding environment to burn its fuel in the combustion chamber. It therefore has much greater specific impulse than a solid propellant rocket motor, and this also results in greater range and higher speed. As opposed to a gas turbine engine, a ramjet needs no moving parts to compress the air and relies solely on its forward motion. However, it therefore requires a means of boosting itself to supersonic speed, usually with a small rocket motor, so that it can make sufficient thrust to accelerate.

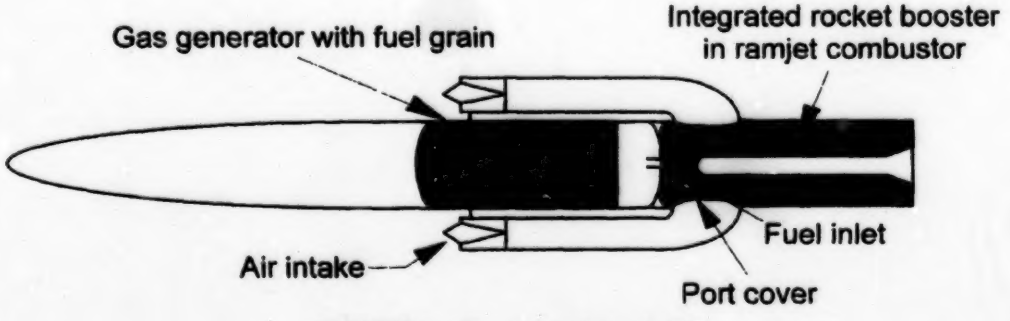

FIGURE 1 – Ducted rocket missile

A solid fuel ducted rocket is a special type of ramjet that uses a solid fuel gas generator placed ahead of the combustion chamber. This fuel, sometimes mixed with a small amount of solid oxidizer to help it react, decomposes to provide a fuel-rich exhaust that is then injected into the ramjet combustor. There the exhaust mixes with the air from

the intakes, burns, and then accelerates through the nozzle to provide thrust. Since the gas generator is separated from the ramjet combustor, throttling is also possible with only a limited increase in complexity over a solid rocket.

3.0 WATER TUNNEL AND OPTICAL SETUP

Water tunnels are frequently used to visualize the non-reacting flowfield within various types of model combustors. As previously mentioned, by using a model geometry at the same scale as the actual combustor but using water as the working fluid instead of gases, the Reynolds number of the flowfield inside the water tunnel (10^5) is representative of that inside the actual combustor (10^6). However, flow velocities are two orders of magnitude less than those in an actual combustor, and visualization of the flowfields by various optical methods is greatly simplified.

The water tunnel used at DREV is essentially a 560 *l* plexiglass tank (Fig. 2). A 2HP pump circulates the water through this closed system at up to 8 *l*/s. Inside the tank is mounted the 100-mm diameter model combustor in the particular geometry of interest (Fig. 3). The tank is completely filled with water so as to minimize optical distortion of images within the model combustor due to refraction. The tank is divided into two parts by a barrier that inhibits "exhaust" water from the model, polluted with the fuel seeding, from obscuring the view of the combustor.

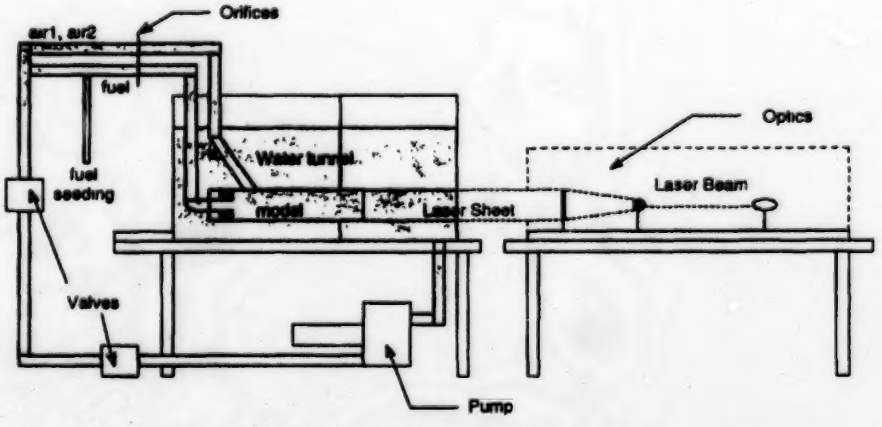

FIGURE 2 - Water tunnel and optics setup

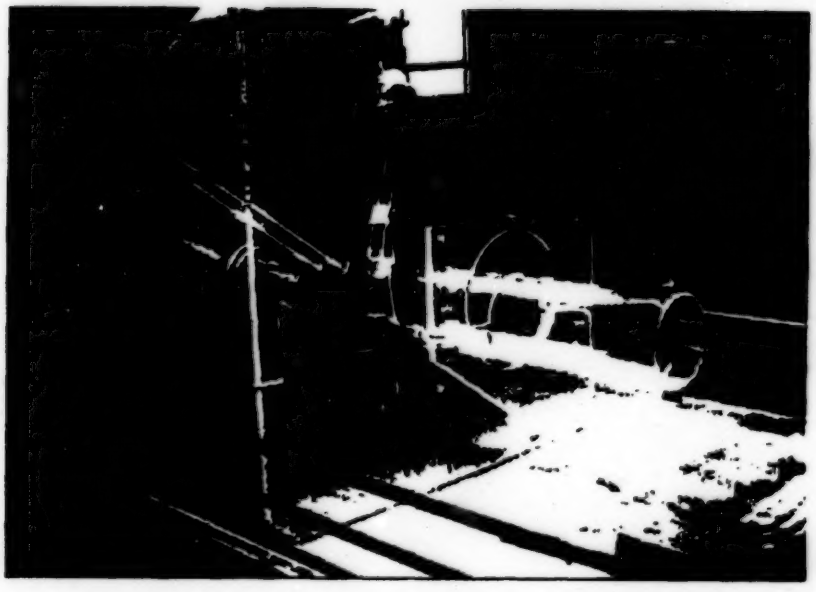

FIGURE 3 - Plexiglass model combustor in water tunnel

Water exiting the pump flows through a master valve that controls the overall flow rate of the whole system. The flow then splits into three pipes, two of which simulate the flow through the air intakes and the other the flow through the fuel inlet. Each pipe is outfitted with its own valve so that the individual flow rates can be precisely controlled. To measure the flow rates, each pipe is equipped with a sharp-edged orifice coupled with a differential pressure transducer. By specifying the flow rate and Reynolds number within the combustor, one can use orifice theory to calculate the desired pressure drop over the orifices to reach a specific momentum ratio. Figure 4 shows a close up of the geometry of the 100-mm diameter combustor model and various fuel inlets. In this project, an A2 air inlet (circular, 38.1 mm diameter, air inlet angle 60 degrees) was used in combination with both the FO-27 and FO-18 fuel inlets. The FO-27 fuel injector has a centrally located 27 mm hole while the FO-18 fuel injector has a centrally located 18 mm hole.

A method to seed the fuel was necessary to distinguish between water that simulated the fuel and the water that simulated the air. While several types of dyes and particles were considered, small gas bubbles were thought to be the best choice since the water tunnel is a closed system and pollution of the recirculating water should be minimized. These bubbles were small enough to faithfully follow the high-speed flow in the combustor, but in the aft part of the tank with very low velocities, they would slowly rise and not be entrained back into the flow.

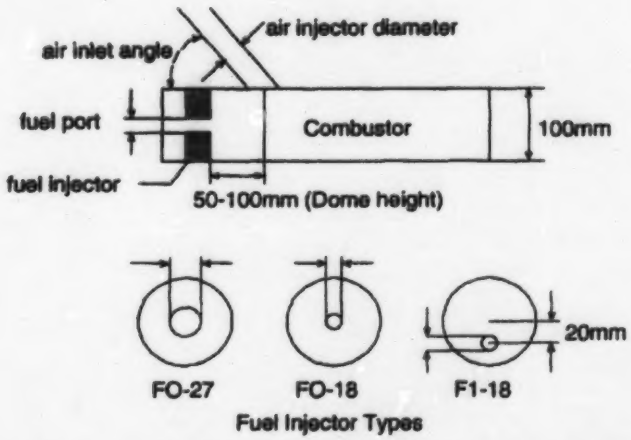

FIGURE 4 - Schematic of plexiglass combustor and fuel injectors

The best way found to seed the flow was to inject a low volume of high-pressure water through a small nozzle mounted just ahead of the orifice on the fuel pipe (Fig. 2). This induced cavitation bubbles with a size distribution that ranged from 20 to 130 microns, with most of the bubbles being about 55 to 60 microns in size. The size range of the cavitation bubbles was measured using an Olympus microscope, model BX50F3, with a 4X objective lens. A Sony camera, model DXC-151A, captured an image of the bubbles and transferred it to a computer via a frame grabber. Image Pro Plus version 4 computer software was then used to calculate the diameter of the approximately sixty bubbles to give a statistically significant size distribution. This size distribution showed that images formed by the bubbles at the CCD of the video camera would be many times smaller than a pixel on the CCD. Since the images of several bubbles could therefore fit on a single

pixel, bubble concentration in the area of the light sheet corresponding to a particular pixel in the CCD was assumed to be proportional to the intensity of light captured by the same pixel.

The optical setup used to visualize the flow phenomena in the model combustor is shown in Fig. 5. A laser sheet was used to illuminate the central, longitudinal plane of the combustor. This particular plane was chosen since it was the symmetry plane of the combustor and, assuming equal flow rates through the air inlets and quasi-steady flow, there is no flow normal to this plane. The optical apparatus used to create this 100 mm high laser sheet consisted of a Spectra-Physics 400-mW krypton-ion laser, three mirrors, a plano-cylindrical lens (30 mm focal length), a collimating plano-convex spherical lens (145 mm diameter, 1000 mm focal length), a beam-steering device and various optical mounts. To ensure maximum power output of the krypton laser beam, the mirrors in the laser cavity were cleaned and aligned. Once the beam left the laser cavity it was redirected by mirror #1 (M1) to the beam-steerer. The beam-steering device consisted of two mirrors and was used to raise the laser beam to the height of the center of the combustor model. Although it might have been easier raising the laser to the correct height, that particular setup was found to be quite unstable therefore it was easier to redirect the beam by use of mirrors to the proper elevation.

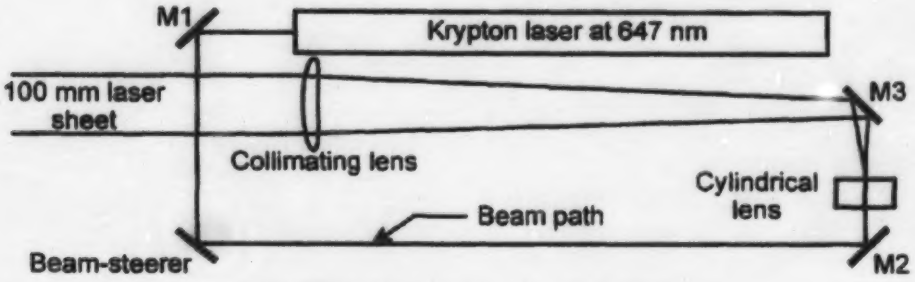

FIGURE 5 - Schematic of optical setup

Once the beam was raised by the beam-steerer, it was passed to mirror #2, which deflected the beam through the cylindrical lens. The cylindrical lens expanded the beam vertically into a sheet that was then deflected by mirror #3 to the collimating lens. The

collimating lens was set at its focal length, 1000 mm, away from the cylindrical lens so that the sheet was collimated properly. When the sheet left the collimating lens, it was passed into the combustor model and aligned with the central plane of the combustor. To reduce the effect of the Gaussian profile of the laser beam, only the middle of the laser sheet was used. There was still a slight intensity loss at the edges of the remaining sheet, but not nearly as much as there could have been had the sheet not been diverged to a larger size than the model. The light scattered off the bubbles in this sheet inside the model combustor was captured as an sequence of images by a Sony DCR-VX700 digital video camera and transferred to a computer through a miroVIDEO DC20 frame-grabber.

4.0 DETERMINATION OF MASS FLOW RATES

As previously mentioned, the water tunnel study included two different geometries, and each of these two geometries was tested at various air and fuel mass flow rates. Since these mass flow rates, and in particular the air/fuel momentum ratio, are important parameters for characterizing the flowfield, each pipe was equipped with an orifice over which the drop in pressure was measured to obtain the flow rate within each pipe. Figure 6 shows a schematic diagram of an orifice and a section of pipe, located much further downstream, that narrows to the injector size.

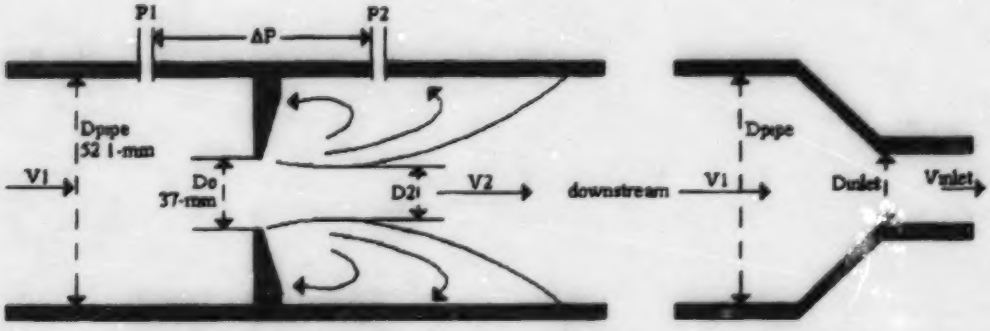

FIGURE 6 – Schematic of a pipe orifice

Bernoulli's equation for incompressible flow (Ref. 3) through the orifice follows:

$$P_1+\rho V_1^2/2=P_2+\rho V_2^2/2 \quad [1]$$

where ρ is the density of water, P_1 is the pressure before the orifice, P_2 is the pressure after the orifice, V_1 is the velocity well upstream of the orifice, and V_2 is the velocity at the narrowest point of the jet downstream of the orifice as shown in Fig. 6. The pressure drop is given by:

$$\Delta P=P_1-P_2=\rho/2(V_2^2-V_1^2) \quad [2]$$

Given the contraction coefficient, $C_c=A_2/A_o$, where A_0 is the area of the orifice and A_2 is the minimum area of the jet after the orifice, it is possible to relate the velocities, V_1 and V_2, as follows:

$$V_1A_1=V_2C_cA_o \quad [3]$$

And the velocities further downstream at the narrowing are related similarly:

$$V_1A_1=V_{inlet}A_{inlet} \quad [4]$$

By eliminating all the unknown variables and solving for ΔP, one can obtain an expression for the drop in pressure as a function of inlet velocity and inlet diameter:

$$\Delta P=\rho/2V^2_{inlet}(D_{inlet}/D_{pipe})^4(1/C_c^2(D_{pipe}/D_o)^2-1) \quad [5]$$

where D_{inlet} is the diameter of the inlet pipe to the combustor model, D_{pipe} is the diameter of the pipe in which the orifice is installed, and V_{inlet} is the velocity through the inlet. Substituting in values for the known diameters, the density of water (1000 kg/m^3) and C_c=0.65943, a more understandable formula is reached:

$$\Delta P=5.45655X10^{10}*V^2_{inlet}D^4_{inlet} \quad [6]$$

The mass flow, kg/s, in each pipe is given by the following formula

$$m=\rho Q=\rho V_{inlet}A_{inlet} \quad [7]$$

where Q (m^3/s) is the discharge from the inlet. The critical factor in describing a flowfield is the air to fuel momentum ratio where the momentum is defined as the product of the mass flow and velocity in the inlet:

$$\text{Momentum Ratio}=2m_{air}V_{air}/m_{fuel}V_{fuel} \quad [8]$$

The factor of two in the above formulas arises due to the fact that there are two air inlets emptying into the model combustor.

Another important factor in describing the flow is the Reynolds number. This quantity determines whether the flow will be turbulent or laminar. The Reynolds number in the combustor is given by:

$$R_{combustor}= \rho D_c V_c/\mu \quad [9]$$

where μ is the kinematic viscosity of water, D_c is the diameter of the combustor and V_c is the velocity in the combustor. It is easier to specify the Reynolds number in the combustor in terms of mass flow from each inlet since mass flow is conserved and is also a scalar quantity, unlike velocity. After some manipulation and use of the relation given in Eqn. 7, Eqn 9 takes the following form:

$$R_{combustor}=4(2m_{air}+m_{fuel})/\mu\pi D_c \quad [10]$$

5.0 CFD MODELLING

Computational fluid dynamics (CFD) modelling of the same geometries and air/fuel momentum ratios studied in the water tunnel was carried out using a code known as FLUENT (Version 4.4) from FLUENT, Inc. Meshes of the exact geometries used in the water tunnel were generated with a preprocessor called GEOMESH (Version 3) also from FLUENT Inc. The volumes were discretized into structured grids of approximately 100,000 hexahedral cells, of which only half were live cells lying within the combustor shown in Fig. 7 (the rest were dead cells lying outside the combustor geometry but required to complete the structured mesh). Since water was the working fluid, the

properties of water at 25°C were used and an incompressible fluid was assumed. The boundary conditions present in the actual water tunnel tests were estimated and used as inputs for the modelling and, in each case, the Renormalized Group Theory (RNG) turbulence model was used.

The fundamental difference between the CFD modelling and the images taken from the water tunnel tests was that FLUENT, with the RNG turbulence model, is a quasi-steady modelling code based on the time-averaged (Reynolds averaged) Navier-Stokes equations. Turbulent flow is highly time-dependent, but using CFD with a turbulence model results in a time-averaged result for the flow phenomena, so this time-dependence is not evident. However, each video image from the water tunnel is actually a "snapshot" of the flow, averaged only over the duration the shutter of the camera is open, and the time dependency of the flow can be easily seen. To overcome this difference between the water tunnel and CFD results, a final image correction technique was devised to take ten sequential video images from each test. These images were then averaged to get a less time-dependent view of the flowfield. While hundreds of images would be necessary to get a statistically accurate averaged flowfield, the computer resources available limited the practical number of images that could be averaged.

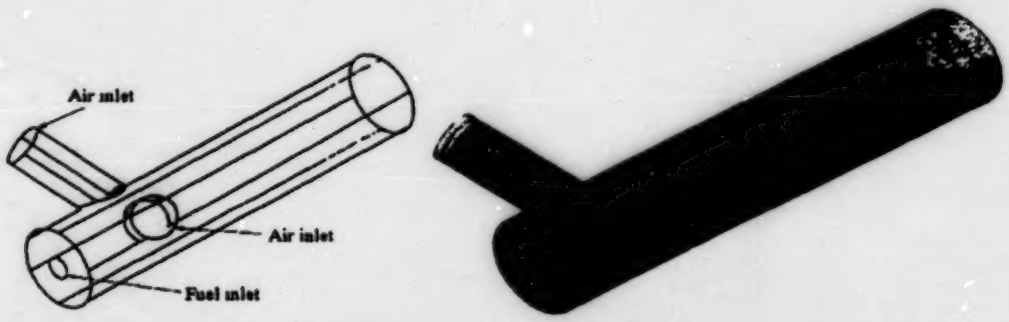

FIGURE 7 - Schematic and surface mesh of the basic combustor geometry

6.0 FINAL IMAGE CORRECTION TECHNIQUE

To make the fuel concentrations in the water tunnel images directly comparable to the results from the CFD modelling, some correction to the raw images was required. The purpose of these corrections was to have the bubble or simulated fuel concentration as directly proportional to the intensity of light landing on each pixel as possible. To do this, the raw images needed to be corrected mainly for the effects of Mie scattering and for the intensity variations of the laser sheet due to attenuation and the Gaussian profile of the laser beam as previously mentioned. They were not corrected for optical distortion, reflections, nor the effects of multiple scattering. Figure 8 shows a raw image of 100% simulated fuel, where both air inlet valves were closed and water, with the seeding from the cavitation bubbles, flowed only through the fuel inlet. The image was taken with a digital video camera that was stationed at a 90-degree angle with respect to the combustor model. Graph #1 in Fig. 8 shows the variation in horizontal pixel intensity versus pixel number from the left-hand side to the right-hand side of the 100% fuel image at the midpoint of the image. As stated previously, this horizontal intensity variation is mainly

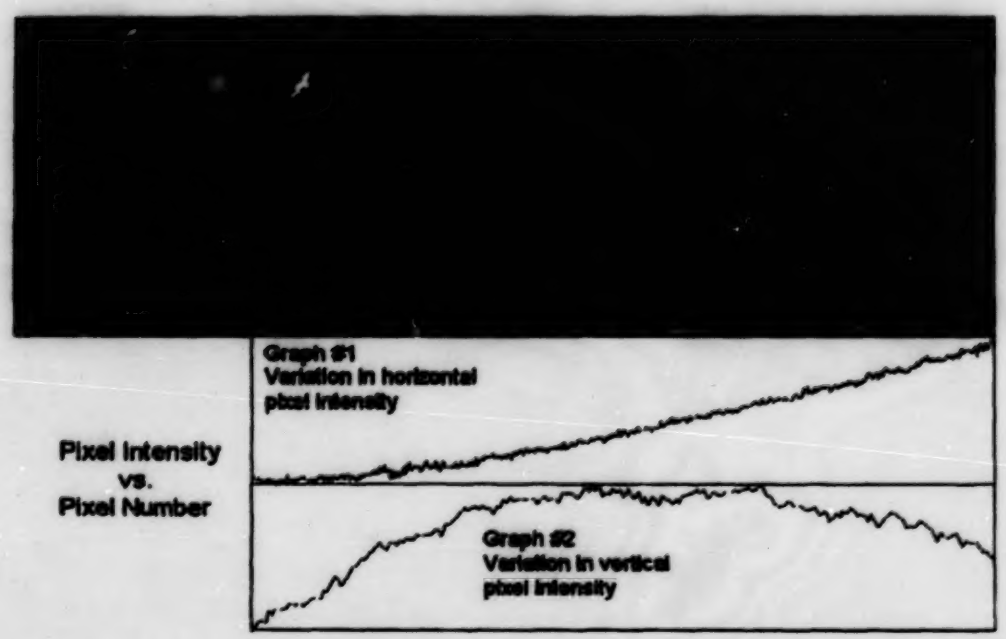

FIGURE 8 – 100% fuel image with vertical and horizontal plot profiles

due to the fact that the amount of laser light scattered in the forward direction by the fuel seeding is many times greater than the light scattered in the backward direction by the fuel seeding. The laser sheet is also attenuated as it passes through the sheet. Graph #2 shows the variation in pixel intensity versus pixel number from the top of the 100% fuel image to the bottom, once again at the midpoint of the image. This vertical variation is mainly due to the Gaussian profile of the laser sheet.

To overcome these variations in intensity, a final image correction technique was developed that corrected each image pixel by pixel. A FORTRAN computer program was written to read each image and correct for the horizontal and vertical variations mentioned earlier. The corrected images were then rescaled using the pixel intensity values at areas on the image known to be essentially 0% and 100% fuel so that pixel intensity would be proportional to the fuel concentration. Figure 9 shows false color representations of the 100% fuel image shown previously in Fig. 8. The image to the left is completely uncorrected while the image on the right has undergone vertical and horizontal correction but has not been rescaled. As can be seen, except for the area in the upper left corner due to reflections from the air inlet pipe intersecting the combustor, the fuel concentration in the corrected fuel image is of greater uniformity than in the uncorrected image. Upon rescaling, the corrected 100% fuel image should exhibit more accurate fuel concentrations for quantitative comparison with the CFD results.

FIGURE 9 – False colour comparison of the uncorrected 100% fuel image to the corrected 100% fuel image

Another matter to be considered was the fact that the images from the water tunnel were time dependent while the CFD modelling results were quasi-steady. To reduce this time dependence, ten corrected, sequential images taken at 15 frames per second were

added pixel by pixel to output an average image. This time-independent, average image was then used for direct comparison with the CFD modelling with FLUENT.

7.0 REYNOLDS NUMBER EFFECTS

The validity of the water tunnel tests to reproduce the non-reacting flowfield with an actual combustor depends on whether there is any dependence on Reynolds number. If not, the flow observed in the model combustor of the water tunnel should be representative of the much higher Reynolds number flowfield found in the actual combustor, ignoring any compressibility effects. Figure 10 shows two sets of fully corrected and averaged water tunnel images taken using the same combination of air injector, fuel injector, and air/fuel momentum ratio at two different Reynolds numbers. As one can see, the shapes of the fuel plumes are quite similar and, considering any error due to not averaging hundreds of images, there is no evidence of Reynolds number dependence on the size and shape of the fuel jets.

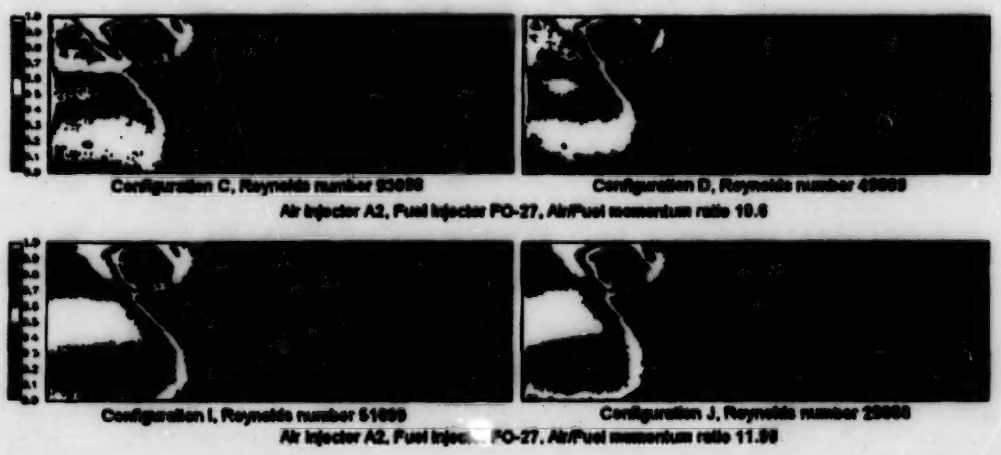
Configuration C, Reynolds number 93000
Configuration D, Reynolds number 49000
Air Injector A2, Fuel Injector PO-27, Air/Fuel momentum ratio 10.6
Configuration I, Reynolds number 51000
Configuration J, Reynolds number 23000
Air Injector A2, Fuel Injec... PO-27, Air/Fuel momentum ratio 11.56

FIGURE 10 – Corrected and averaged comparisons to show Reynolds number independence

8.0 WATER TUNNEL AND CFD COMPARISON

References 1 and 2 detail previous water tunnel studies of various combinations of geometry and test conditions for the ducted rocket combustor, but for these studies no image correction was carried out. Comparisons between the water tunnel images and CFD results were therefore qualitative. To evaluate the image correction technique for the present study, two different geometries were chosen from the earlier tests. They included two different fuel injectors having single central ports of 18 mm diameter (designated FO-18) and 27 mm diameter (designated FO-27), a 38.1 mm diameter air injector with an air inlet angle of 60 degrees (designated A2), and a dome height of 57 mm. Seven momentum ratios were investigated and, for the FO-27 inlet, were modelled at two different Reynolds numbers to make 12 possibilities. A summary of the test conditions and configurations completed using the water tunnel are listed in Table I. Once each test has undergone the image correction technique and averaged to produce a final image, it was compared to the CFD modelling of identical boundary conditions.

TABLE I

Configurations for water tunnel and CFD modelling

Test	Air inlet	Fuel inlet	Air velocity [m/s]	Fuel velocity [m/s]	Air/fuel mass flow ratio	Air/fuel momentum ratio	Reynolds Number combustor
A	A2	FO-27	2.5	2.167097	4.59	5.3	98198
B	A2	FO-27	1.25	1.083548	4.59	5.3	49099
C	A2	FO-27	2.5	1.532369	6.5	10.6	93058
D	A2	FO-27	1.25	0.766184	6.5	10.6	46529
E	A2	FO-27	2.5	1.097618	9.07	20.66	89536
F	A2	FO-27	1.25	0.548809	9.07	20.66	44768
G	A2	FO-27	1.4	1.602387	3.48	3.04	58141
H	A2	FO-27	0.7	0.801194	3.48	3.04	29070
I	A2	FO-27	1.4	0.80719	6.91	11.98	51699
J	A2	FO-27	0.7	0.403595	6.91	11.98	25850
K	A2	FO-18	1.4	2.4276	5.17	2.98	53901
L	A2	FO-18	2.5	2.2985	9.75	10.6	88920

Figure 11 compares an averaged and corrected water tunnel image from configuration A with a contour plot of fuel mass fraction (or volume fraction since the densities of the simulated "air" and "fuel" are assumed to be identical) on the central, longitudinal plane from the CFD modelling. The fuel mass fraction legend is shown to the left where the areas of highest fuel concentration are the lightest-colored areas for both the water tunnel image and the CFD modelling. There is agreement between the shapes and concentrations of the fuel plumes between the water tunnel image and the CFD modelling. However, further downstream in the combustor region of the experimental image there seems to be a much higher fuel concentration that is inconsistent with the CFD modelling.

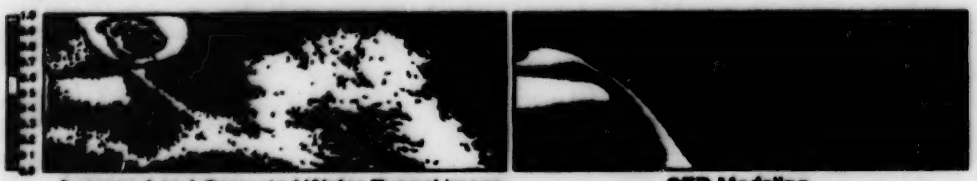

FIGURE 11 – Configuration A, Air injector A2, Fuel injector FO-27, Air/Fuel momentum ratio 5.3, Reynolds number 98198

Figure 12 shows configuration B, which was taken under identical conditions as for Fig. 11, but at a different Reynolds number. Again, the shape of the fuel jet agrees quite well, but there is still some high, downstream fuel concentrations in the experimental image that do not compare favorably with the CFD modelling under these conditions.

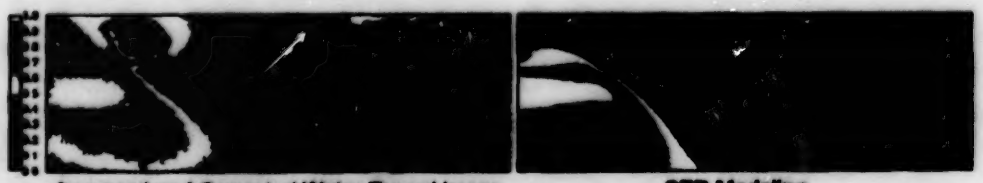

FIGURE 12 – Configuration B, Air injector A2, Fuel injector FO-27, Air/Fuel momentum ratio 5.3, Reynolds number 49099

Configuration C, shown in Fig. 13, was taken under the same conditions as for configuration A and B, but at an air/fuel momentum ratio that was twice as high. As expected, the fuel jet is shortened and turned back into the dome region of the combustor

more than in the images for configurations A and B. This comparison exhibits excellent agreement between the fuel concentrations throughout the whole combustor with the exception that the fuel jet in the experimental image appears slightly less intense, and could probably be rescaled better.

FIGURE 13 – Configuration C, Air injector A2, Fuel injector FO-27, Air/Fuel momentum ratio 10.6, Reynolds number 93058

Figure 14 shows configuration D, which is identical to configuration C but at half the Reynolds number. The fuel jet is also shortened and turned back as first shown in configuration C. Upon comparison with the CFD modelling to the right, the experimental image also demonstrates good agreement of fuel concentration throughout the entire combustor.

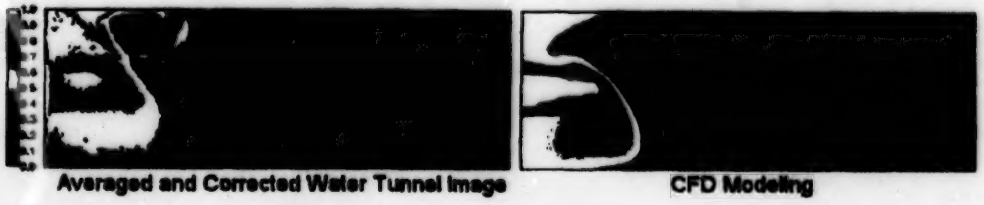

FIGURE 14 – Configuration D, Air injector A2, Fuel injector FO-27, Air/Fuel momentum ratio 10.6, Reynolds number 46529

Configuration E, shown in Fig. 15, uses the same air and fuel injectors as used in the previous tests, but was taken at an even higher air/fuel momentum ratio. The fuel jet is further shortened and turned back than was found in the experimental images of configurations C and D. The experimental water tunnel image seems slightly unstable, but agrees somewhat with the shape of the fuel jet in the CFD modelling. Also the fuel concentrations of the fuel jet agree, but again there is a higher fuel concentration in the main combustor region.

FIGURE 15 – Configuration E, Air injector A2, Fuel injector FO-27, Air/Fuel momentum ratio 20.66, Reynolds number 89536

Again, configuration F in Fig. 16 shows the same configuration as configuration E, but at a lower Reynolds number. In this image, it is much easier to see the fuel jet being turned back into the dome region than in the experimental image for configuration E. Upon comparison of the experimental image to the CFD modelling, one can see excellent agreement between the shape of the fuel jet and fuel concentrations throughout the entire combustion chamber.

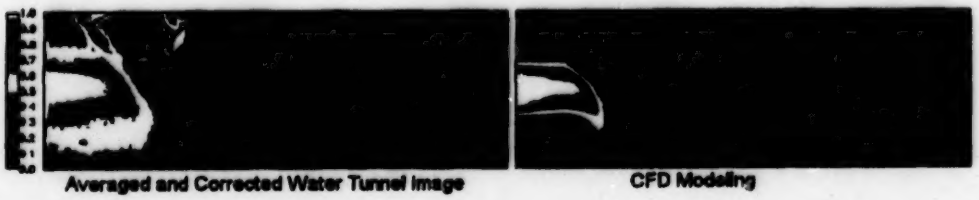

FIGURE 16 – Configuration F, Air injector A2, Fuel injector FO-27, Air/Fuel momentum ratio 20.66, Reynolds number 44768

Configuration G, in Fig. 17, illustrates the flowfield with the same air and fuel injectors but a low air/fuel momentum ratio. The fuel jet impinges farther into the air inlet region than for a higher air/fuel momentum ratio, as one would expect with a relatively

FIGURE 17 – Configuration G, Air injector A2, Fuel injector FO-27, Air/Fuel momentum ratio 3.04, Reynolds number 58141

higher fuel momentum. The form of the main fuel jet agrees fairly well with the CFD, but the fuel concentrations within the dome region appear to be over-corrected with respect to the CFD results. Figure 18 exhibits the same behaviour.

Configuration H, in Fig. 18, is taken under identical conditions as for configuration G, but again at half the Reynolds number. The fuel jet also exhibits agreement with the CFD modelling, but as mentioned in the previous paragraph, the fuel concentration in the dome head looks slightly off maybe due to an over-correction factor.

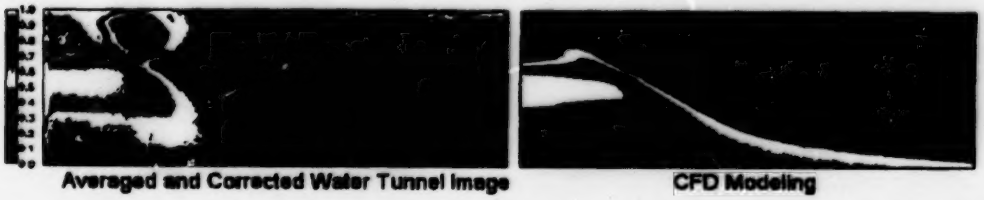

FIGURE 18 – Configuration H, Air injector A2, Fuel injector FO-27, Air/Fuel momentum ratio 3.04, Reynolds number 29070

Figure 19 shows another air/fuel momentum ratio using the A2 air injector and FO-27 fuel injector. This momentum ratio is similar to that of configuration C, so the images exhibit comparable behavior such as the fuel jet being turned back into the head of the combustor. For this configuration, the fuel concentrations in the experimental image are higher in the dome region than for the CFD modelling, but are in good agreement downstream of the air inlets.

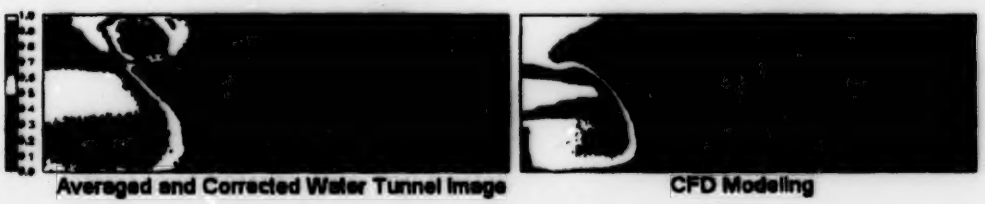

FIGURE 19 – Configuration I, Air injector A2, Fuel injector FO-27, Air/Fuel momentum ratio 11.98, Reynolds number 51699

Configuration J, shown in Fig. 20, is identical to that of configuration I but the Reynolds number in the combustor is halved. The experimental image also exhibits agreement near the fuel and air injectors but further downstream there is a slightly higher fuel concentration than with the CFD modelling.

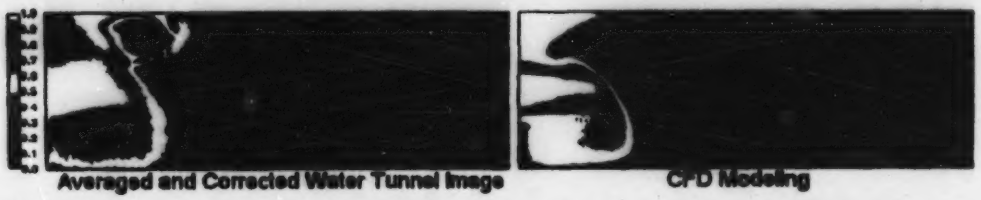

FIGURE 20 – Configuration J, Air injector A2, Fuel injector FO-27, Air/Fuel momentum ratio 11.98, Reynolds number 25850

Figure 21 shows configuration K, which uses the FO-18 fuel injector and the A2 air injector. The air/fuel momentum ratio is quite low, so the image is comparable to configurations G and H with the only variation being the fuel injector. The FO-18 injector has a smaller inlet that leads to a higher fuel velocity from the fuel inlet. As one can see, the experimental water tunnel image in Fig. 21 demonstrates this behaviour by having a fuel jet that penetrates further into the air inlet region than it did for the larger diameter fuel injector. The shape and fuel concentrations of the water tunnel image and the CFD modelling agree fairly well.

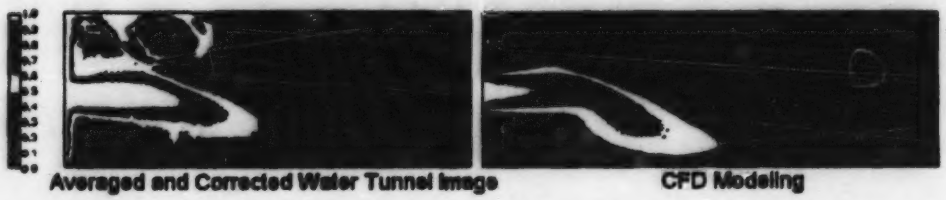

FIGURE 21 – Configuration K, Air injector A2, Fuel injector FO-18, Air/Fuel momentum ratio 2.98, Reynolds number 53901

Configuration L, also using the FO-18 fuel injector and A2 air injector, is shown in Fig. 22. This configuration has an identical air/fuel momentum ratio as for configurations C and D, with the only difference being the fuel injector. As mentioned earlier, the smaller fuel injector leads to a higher fuel inlet velocity, so that fuel jet will

penetrate further into the air inlet region than with a larger fuel injector. Agreement between the experimental image and the CFD modelling for the shape of the fuel jet and fuel concentrations is good.

FIGURE 22 – Configuration L, Air injector A2, Fuel injector FO-18, Air/Fuel momentum ratio 10.6, Reynolds number 88920

The general tendency seen, once all the results are considered, was that better agreement was obtained between the water tunnel images and CFD results for the configurations that had higher air/fuel mass flow ratios. This may have been since the flow rate of the high-pressure water to create the seeding was constant. If the seeding rate were constant, there would have been more contrast between the simulated air and fuel streams for the higher air/fuel mass flow ratios. This is consistent with the fact that the image for each low Reynolds number configuration appeared to give better results than the corresponding high Reynolds number configuration. Further improvements should therefore be made to the seeding and correction techniques to ensure more consistent results. However, results were good for some of the configurations. If these improvements are made and allowances are made for the inaccuracies modelling the flow with CFD, this water tunnel image correction technique could be a useful tool to quantitatively validate CFD results for ducted rocket and other types of combustors.

9.0 CONCLUSIONS AND RECOMMENDATIONS

Based on information found in previous studies, a water tunnel was used to model ducted rocket propulsion. Twelve different geometries and test conditions were investigated and compared with CFD modelling of similar boundary conditions. The results found in prior experiments were mainly qualitative due to the fact that several optical phenomena hindered the comparisons. An improved image correction technique was developed to

reduce the effect of these optical phenomena and allow for more quantitative comparisons of fuel concentration with the CFD results.

Modifications to the optical setup reduced the vertical intensity variation of the laser sheet and greatly improved the results. These modifications included the addition of a 145 mm diameter spherical lens to recollimate the laser beam and the use of only middle of the laser sheet.

An image-processing program, written in FORTRAN, was created to correct the raw images vertically (laser sheet intensity) and horizontally (Mie scattering) for the variations in the laser sheet used to visualize the flow in the central, longitudinal plane of the combustor. Basically, this program made the bubble concentration in the model directly proportional to the pixel intensity and rescaled the corrected images from 0 to 100% fuel.

The images were not corrected for reflections, optical distortion, nor multiple scattering. The reflections are evident on all the water tunnel images and were simply ignored during the comparisons. Effects from optical distortion and multiple scattering were considered to be small.

To overcome the time-dependence of the flow phenomena, ten sequential, corrected and rescaled images were averaged to be more comparable to the quasi-steady CFD images produced by FLUENT. These averaged images provide a quantitative fuel concentration comparison with CFD modelling.

In all the water tunnel tests performed, no real evidence of Reynolds number dependence was found. Allowing for the effects of increased seeding of the fuel stream at lower Reynolds numbers and the fact that an averaged image is not completely independent of time, all the images modelled at the same air/fuel momentum ratio were similar and exhibited the same flow behaviour. Therefore, the flowfields visualized at the Reynolds numbers in the water tunnel should be representative of the higher Reynolds number

flowfields found in actual ducted rocket combustors, if compressibility effects can be neglected.

Better agreement was obtained between the water tunnel images and CFD results for the configurations that had higher air/fuel mass flow ratios. This was likely related to the seeding technique. This is consistent with the fact that the image for each low Reynolds number configuration appeared to give a better comparison with the CFD results than did the image for the corresponding high Reynolds number configuration.

Further improvements should be made to the seeding and correction techniques to ensure more consistent results. With these improvements and allowances for the inaccuracies modelling the flow with CFD such as estimating boundary conditions and assuming quasi-steady flow, this water tunnel image correction technique could be a useful tool to quantitatively validate CFD results of various combustors.

10.0 ACKNOWLEDGEMENTS

The authors would like to thank everyone at DREV who contributed to the operation of the water tunnel, particularly the personnel of the Propulsion Group. They also gratefully acknowledge the help of Grant McIntosh of Weapons Effects with the image processing program, and also Charles Dubois, Michel Hébert and Rémy Coulombe for their ideas and contribution to determining the size of the cavitation bubbles used for the fuel seeding.

11.0 REFERENCES

1. Stowe, R.A., De Champlain, A., Mayer, A.E.H.J, and Niemeijer, S.F., "Modelling and Water Tunnel Visualization of Air/Fuel Mixing in a Ducted Rocket Combustor", IRRDP-DREV/TNO-TN-9707(1), DREV-TM-9828, February 1999, UNCLASSIFIED

2. Neimeijer, S.F., "A Water Tunnel Investigation of Air/Fuel Mixing in a Ducted Rocket Combustor", Thesis for Aeronautical Engineering degree at the Haarlem Polytechnic School, Haarlem, the Netherlands, June 1997

3. Streeter, V.L. and Wylie, E.B., "Fluid Mechanics", 7th Edition, McGraw-Hill, 1979.

UNCLASSIFIED

INTERNAL DISTRIBUTION

DREV TM 1999-220

1	-	Director General
1	-	Deputy Director General
1	-	Chief Scientist
6	-	Document Library
1	-	Head, Delivery Systems
1	-	Head, Energetic Materials Section
1	-	Head, Weapon Effects Section
1	-	Head, Electro-Optical Warfare Section
1	-	Mr. R.A. Stowe (author)
1	-	Mr. P. Harris
1	-	Mr. M. Lauzon
1	-	Mr. C. Dubois
1	-	Mr. F. Lesage
1	-	Dr. J. Rapanotti
1	-	Mr. R. Farinaccio
1	-	Dr. L.-S. Lussier

UNCLASSIFIED

EXTERNAL DISTRIBUTION

DREV TM 1999-220

1	-	DRDCIM
1	-	DRDCIM (unbound copy)
1	-	DRDB
1	-	DSTM
1	-	DSTL
1	-	DSTA
1	-	DAR 5
1	-	DAEPM (FT) 5-4
1	-	DAEPM (FT) 3-4
1	-	DAEPM (FT) 3-2
1	-	Marlene Jeffries (author)
1	-	Dr. A. De Champlain Département de génie mécanique Université Laval
1	-	Royal Military College of Canada Department of Mechanical Engineering Attn: Dr. M.F. Bardon
1	-	Carleton University Dept. of Mechanical and Aerospace Engineering Attn: Dr. J.E.D. Gauthier
1	-	Bristol Aerospace Ltd. Missile Engineering Department
4	-	TNO Prins Maurits Laboratory Group Rocket Technology Attn: Mr. R. Calzone
1	-	TNO Prins Maurits Laboratory (unbound copy) Group Rocket Technology Attn: Mr. R. Calzone

DOCUMENT CONTROL DATA

1. ORIGINATOR (name and address) Defence Research Establishment Valcartier 2459 Pie XI Blvd North Val-Bélair, QC G3J 1X5	2. SECURITY CLASSIFICATION (including special warning terms if applicable) Unclassified

3. TITLE (its classification should be indicated by the appropriate abbreviation (S, C, R or U)
Improved Image Correction Technique for Visualization of the Air/Fuel Mixing in a Ducted Rocket Combustor

4. AUTHORS (Last name, first name, middle initial. If military, show rank, e.g. Doe, Maj. John E.)
Jeffries, M.A. and Stowe, R.A..

5 DATE OF PUBLICATION (month and year)	6a. NO. OF PAGES	6b. NO. OF REFERENCES
February 2000	30	3

7. DESCRIPTIVE NOTES (the category of the document, e.g. technical report, technical note or memorandum. Give the inclusive dates when a specific reporting period is covered.)
DREV Technical Memorandum

8. SPONSORING ACTIVITY (name and address)

9a. PROJECT OR GRANT NO. (Please specify whether project or grant)	9b. CONTRACT NO.
3eb13	

10a. ORIGINATOR'S DOCUMENT NUMBER	10b. OTHER DOCUMENT NOS
DREV TM 1999-220	N/A

11. DOCUMENT AVAILABILITY (any limitations on further dissemination of the document, other than those imposed by security classification)

- [x] Unlimited distribution
- [ ] Contractors in approved countries (specify)
- [ ] Canadian contractors (with need-to-know)
- [ ] Government (with need-to-know)
- [ ] Defense departments
- [ ] Other (please specify)

12. DOCUMENT ANNOUNCEMENT (any limitation to the bibliographic announcement of this document. This will normally correspond to the Document Availability (11) However, where further distribution (beyond the audience specified in 11) is possible, a wider announcement audience may be selected.)

13. ABSTRACT (a brief and factual summary of the document. It may also appear elsewhere in the body of the document itself. It is highly desirable that the abstract of classified documents be unclassified. Each paragraph of the abstract shall begin with an indication of the security classification of the information in the paragraph (unless the document itself is unclassified) represented as (S), (C), (R), or (U). It is not necessary to include here abstracts in both official languages unless the text is bilingual).

The Defence Research Establishment Valcartier (DREV) in Canada and the TNO Prins Maurits Laboratory (TNO-PML) in the Netherlands have undertaken a collaborative activity known as the Integral Rocket Ramjet Demonstration Program (IRRDP) to demonstrate several of the key technologies of an airbreathing propulsion unit for a medium-range air-launched missile. An essential component of the airbreathing propulsion system is the ducted rocket combustor and, as part of its development, extensive visualization of the simulated air/fuel mixing has been done using plexiglass models within a water tunnel. Images of simulated fuel concentration were used to validate computational fluid dynamic (CFD) modelling of the same combustor, but unfortunately only qualitative comparisons were possible because of effects from several optical phenomena. Improved optics and image correction techniques to account for the various optical phenomena have yielded more quantitative results of simulated fuel concentration within the combustor. Comparisons of time-averaged, corrected images to the CFD results have been very encouraging for some of the configurations studied.

14. KEYWORDS, DESCRIPTORS or IDENTIFIERS (technically meaningful terms or short phrases that characterize a document and could be helpful in cataloguing the document. They should be selected so that no security classification is required. Identifiers, such as equipment model designation, trade name, military project code name, geographic location may also be included. If possible keywords should be selected from a published thesaurus, e.g. Thesaurus of Engineering and Scientific Terms (TEST) and that thesaurus-identified. If it is not possible to select indexing terms which are Unclassified, the classification of each should be indicated as with the title.)

ducted rocket
water tunnel
Computational Fluid Dynamics
CFD
ramjet
solid fuel
gas generator
mixing
combustor
laser
image correction
video camera
airbreathing propulsion
missile

#513411

dod03e